JETIR.ORG ISSN: 2349-5162 | ESTD Year : 2014 | Monthly Issue
JOURNAL OF EMERGING TECHNOLOGIES AND INNOVATIVE RESEARCH (JETIR)
An International Scholarly Open Access, Peer-reviewed, Refereed Journal

Synthesis and Electrical Characterization of SnO_2–TiO_2 Composite for Enhanced CO_2 Gas Sensor Performance

Sarika R. Bijwe[1] K.B. Raulkar[2]
[1] Department of Physics, Shri Shivaji Science College, Amravati
[2]Department of Physics, Vidya Bharati Mahavidyalaya, Camp, Amravati
Corresponding Author email: *kbraulkar2016@gmail.com*

Abstract:
SnO_2–TiO_2 composite materials were synthesized and investigated for their potential application in CO_2 gas sensing. The structural and electrical properties of the prepared composite were studied to evaluate its sensing characteristics. Incorporation of TiO_2 into SnO_2 modified the electrical conductivity and surface interaction with CO_2 molecules, influencing sensor response. The results demonstrate that the SnO_2–TiO_2 composite exhibits promising characteristics for developing sensitive, stable, and efficient CO_2 gas sensors. P4($40SnO_2$:$60TiO_2$) sensor exhibited the highest sensitivity of approximately 1.33 at 2500 ppm CO_2.

Keywords: SnO_2; TiO_2; SnO_2–TiO_2 composite; CO_2 gas sensor; Gas sensing; Electrical characterization; Sensitivity; Semiconductor metal oxide.

I. Introduction:

Carbon dioxide (CO_2) is an important atmospheric gas whose increasing concentration has created significant concerns in environmental monitoring, industrial processes, indoor air-quality control, and safety applications. Reliable detection and continuous monitoring of CO_2 therefore require sensing materials that provide adequate sensitivity, stability, rapid response, and simple operation. Conventional analytical techniques can provide accurate gas analysis but are often associated with high cost, complex instrumentation, and limited portability. Semiconductor metal oxide (SMO) gas sensors have consequently attracted considerable attention because of their low cost, compact structure, ease of fabrication, and suitability for continuous monitoring [1-2].

Tin oxide (SnO_2) is an n-type semiconductor widely investigated for gas-sensing applications because of its high electrical conductivity, chemical stability, and sensitivity to surface reactions. However, the sensing performance of pristine SnO_2 can be influenced by operating temperature, surface characteristics, humidity, and limited selectivity. Titanium dioxide (TiO_2) is another chemically stable semiconductor with useful surface and catalytic properties. Combining TiO_2 with SnO_2 can modify the surface chemistry, electrical conductivity, defect concentration, and interfacial charge-transfer behavior of the sensing layer. Such interactions can influence adsorption [3-4] of CO_2 molecules and consequently alter the electrical resistance of the sensor. In the present study, an SnO_2–TiO_2 composite was synthesized and its structural and electrical characteristics were investigated to assess its potential for CO_2 gas sensing applications.

II. Experimental

A. Synthesis of SnO_2 Nanoparticles:

GR-grade chemicals (99.99% purity) were obtained from SD Fine, India. SnO_2 nanopowder was synthesized using stannous chloride dihydrate ($SnCl_2 \cdot 2H_2O$). About 2 g of the precursor was dissolved in 100 mL deionized water, followed by the addition of approximately 4 mL ammonia under continuous magnetic stirring. The mixture was stirred for 25 min and allowed to settle for 10–14 h to form a white precipitate. The precipitate was filtered and washed several times with deionized water. Activated carbon (0.27 g) was added, and the mixture was dried at 80 °C for 24 h, powdered, and calcined at 700 °C for 7 h [5].

B. Synthesis TiO_2 Nanoparticles:

TiO_2 nanoparticles were synthesized through the sol–gel method using a suitable titanium precursor. The precursor was dissolved in an appropriate solvent under continuous magnetic stirring to obtain a homogeneous solution. A controlled amount of hydrolyzing agent was then added gradually with constant stirring, resulting in the formation of a stable sol. The sol was aged to promote gel formation and subsequently dried to remove the solvent. The obtained xerogel was ground into fine powder and calcined at an appropriate temperature to produce crystalline TiO_2 nanoparticles.

C. Preparation of thick films:

The screen-printing technique [6] was employed to fabricate thick films of pristine SnO_2, TiO_2, and their composites with different compositions. A thixotropic printing paste was prepared by thoroughly mixing the calcined nanopowders with an organic vehicle containing ethyl cellulose as a temporary binder and suitable solvents, including butyl carbitol acetate and terpineol. The inorganic powder and organic vehicle were maintained in a 75:25 ratio. The prepared pastes were screen-printed onto thoroughly cleaned glass substrates to form uniform thick films [7].

The printed layers were dried at 90–100 °C for 1 h to eliminate the organic constituents. Silver electrodes were subsequently applied to the film surface for electrical measurements and heated at 70 °C for 30 min to ensure proper drying and adhesion. The fabricated SnO_2–TiO_2 composite samples were then used for electrical and CO_2 gas-sensing investigations.

Table 1: Sensor codes

Sr. No.	Sensor codes	Layers
1.	P1	SnO_2
2.	P2	$80SnO_2$: 20 TiO_2
3.	P3	$60SnO_2$: 40 TiO_2
4.	P4	$40SnO_2$: 60 TiO_2
5.	P5	$20SnO_2$: 80 TiO_2
6.	P6	TiO_2

III. Results and Discussions:

A. XRD (X-ray Diffraction) Study:

The XRD patterns [8-9] confirm the crystalline nature of SnO_2–TiO_2 composites, with characteristic reflections of tetragonal rutile SnO_2 and tetragonal anatase TiO_2. Pure SnO_2 exhibits prominent peaks near 26.6°, 33.9°, 37.9°, and 51.8°, corresponding to the (110), (101), (200), and (211) planes. TiO_2 shows anatase reflections, particularly around 25.3°, 37.8°, 48.1°, and 53.9°. The composite patterns retain reflections from both phases, confirming their coexistence without major structural transformation. Increasing TiO_2 content enhances anatase-related reflections. This phase combination can modify surface defects, interfacial charge transfer, and adsorption sites, thereby influencing CO_2 adsorption and the electrical response of the gas sensor.

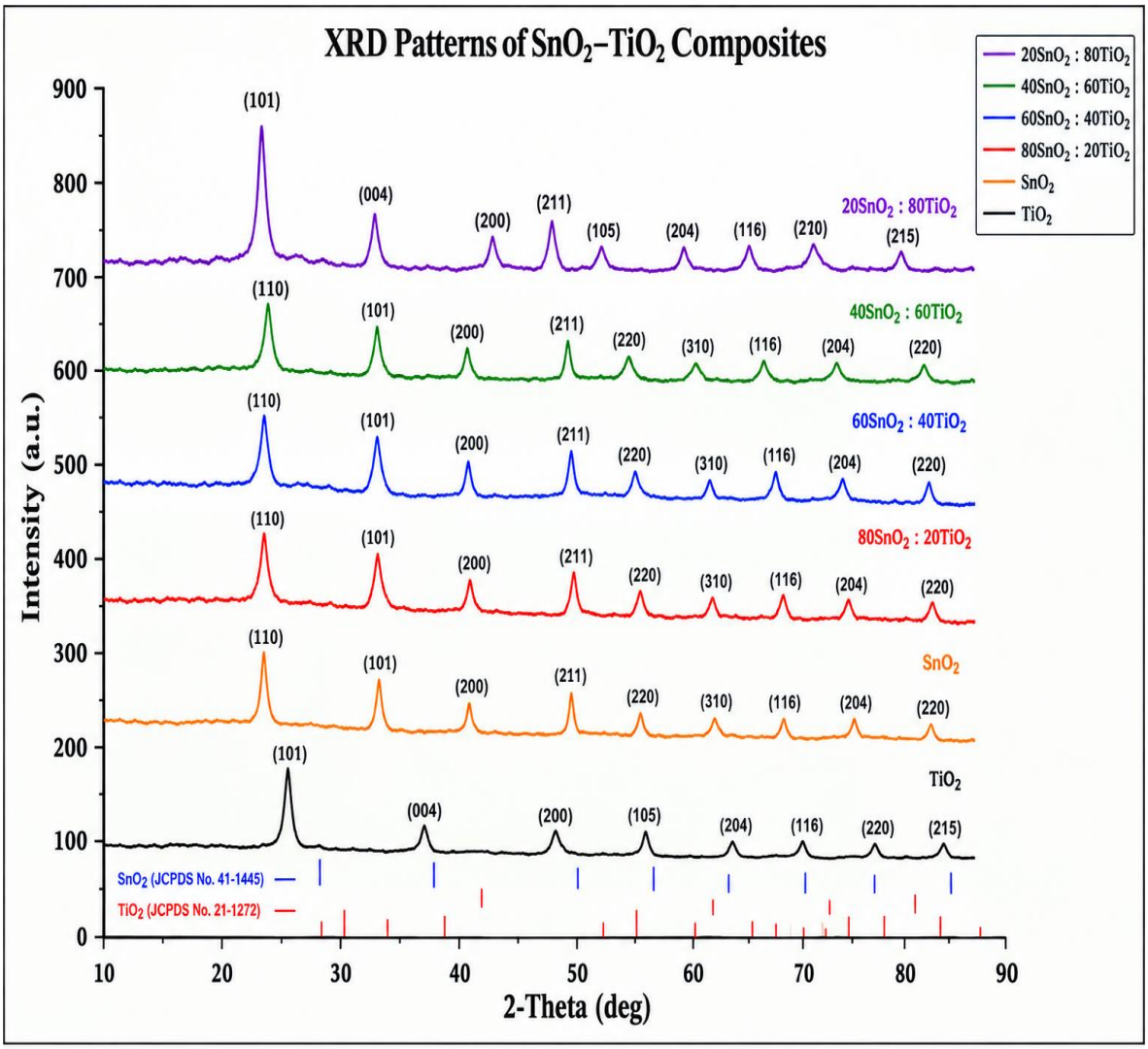

Fig. 1 : XRD pattern of SnO_2+ TiO_2 composites

Table 2: Average crystallite size of SnO_2, TiO_2 and their compositions

Sensor Codes	Chemical Composition of SnO_2: TiO_2 (mole %)	Maximum Intensity Peak Position (2θ) degree	FWHM (2θ) degree	Average Crystallite Size (D) in nm
P1	SnO_2	26.60	0.93	14.7
P2	80SnO_2: 20 TiO_2	26.60	0.92	11.0
P3	60SnO_2: 40 TiO_2	26.62	0.74	9.90
P4	40SnO_2: 60 TiO_2	25.35	0.56	8.78
P5	20SnO_2: 80 TiO_2	25.32	0.94	9.76
P6	TiO_2	24.50	0.70	19.33

The crystallite-size data show that incorporating TiO_2 into SnO_2 progressively reduces the average crystallite size, from 14.7 nm for pure SnO_2 (P1) to 8.78 nm for P4 (40SnO_2:60TiO_2). The smaller crystallite size of P4 can be particularly beneficial for CO_2 gas sensing because it provides a higher surface-to-volume ratio and a greater number of surface-active sites for gas adsorption. The SnO_2–TiO_2 heterointerface can also promote interfacial charge transfer and enhance modulation of electrical resistance during CO_2 adsorption. Thus, the fine crystallite structure of P4 is expected to facilitate stronger surface interaction with CO_2 and contribute to improved sensing performance [10].

B. SEM Study:

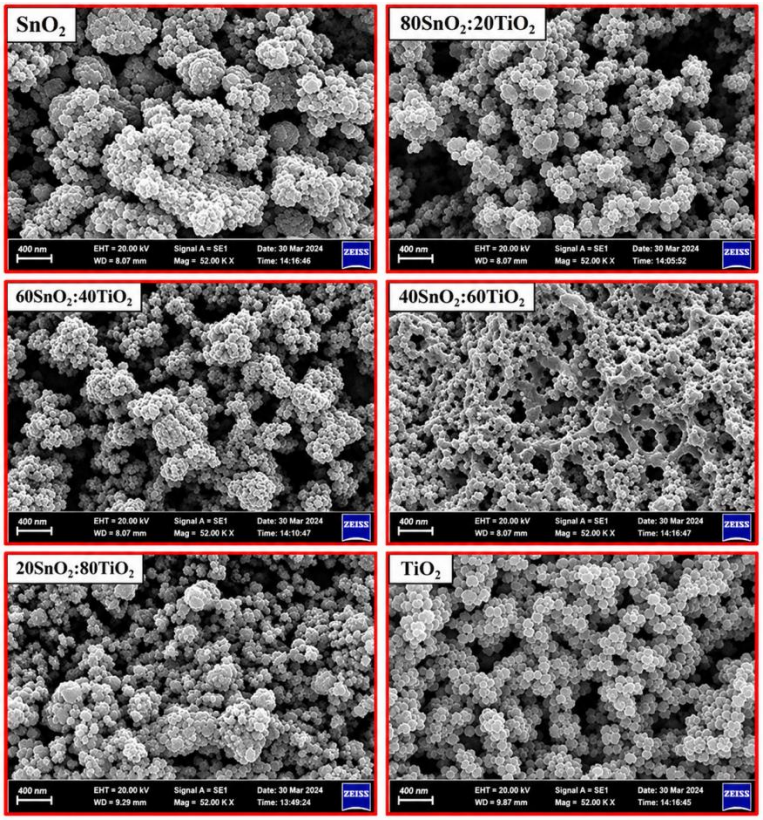

Fig. 2: SEM Pictures of P1 to P6 sensors

The SEM [11-12] micrographs reveal significant morphological changes with TiO_2 incorporation into SnO_2. Among the prepared composites, P4 ($40SnO_2$:$60TiO_2$) exhibits a highly porous and interconnected surface with numerous open pores and fine grains. This porous morphology provides a larger effective surface area and more active sites for CO_2 adsorption. Enhanced gas diffusion through the interconnected pores facilitates greater gas–surface interaction, improving charge modulation and potentially contributing to the enhanced CO_2 sensing response of P4. The porosity, particle size and morphology are listed in table 3.

Table 3: Particle size and morphology of P series.

Sample Code	Composition (SnO_2:TiO_2)	Porosity	Particle Size (nm)	Morphology
P1	SnO_2	Very low	60–100	Low dense
P2	$80SnO_2$:20 TiO_2	Low	50–80	Dense
P3	$60SnO_2$:40 TiO_2	Moderate	40–60	Loosely
P4	$40SnO_2$:60 TiO_2	Very High	20–40	Open, sponge-like porous network
P5	$20SnO_2$:80 TiO_2	High (slightly reduced)	30–50	Polymer-dominant, smoother with embedded particles
P6	TiO_2	Comparatively low	70–110	Slightly low dense

C. Sensitivity measurement:

Sensitivity [13-15] or response of the sensors is measured in terms of change in resistance [16-17] in the environment of CO_2 gas with respect to the resistance of the sensor in air surrounding.
Mathematically, sensitivity is expressed as:

$$S = \left(\frac{R_g - R_a}{R_a} \right) = \left(\frac{\Delta R}{R_a} \right)$$

Where, R_g = sensor resistance in presence of gas
R_a = sensor resistance in the environment of air.

The fabricated sensors showed maximum variations in the resistance at room temperature i.e. 300 K, therefore, the sensivityvity was determined at room temperature.

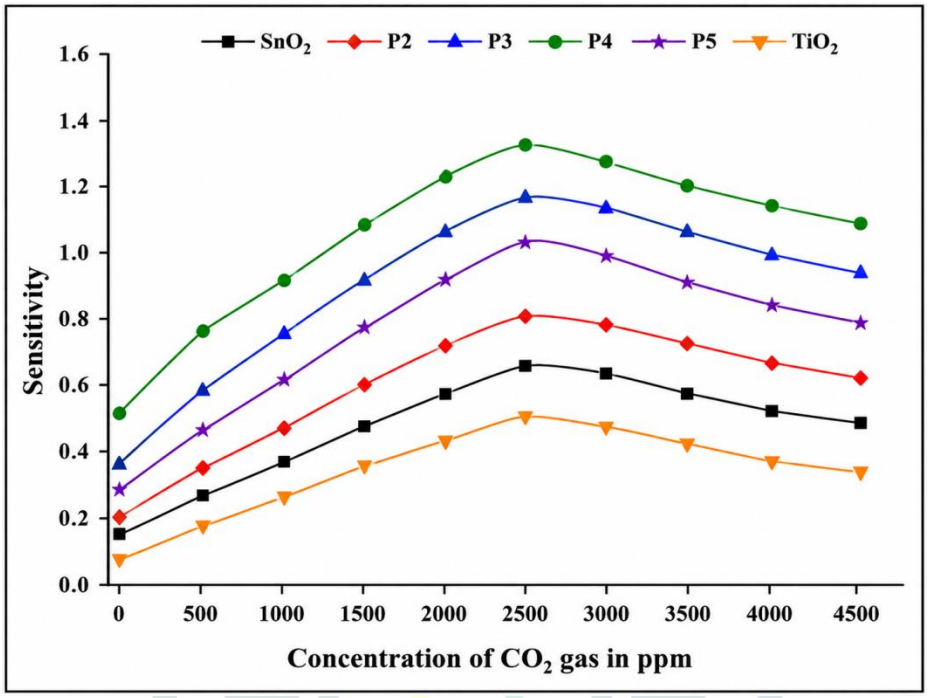

Fig. 3: Variation of sensitivity of P1 to P6 sensors at Room Temperature

The sensitivity response (Fig. 3) of SnO_2–TiO_2 sensors varies significantly with CO_2 concentration. Pure SnO_2 (P1) shows a gradual increase in sensitivity, reaching about 0.65 at 2500 ppm, whereas TiO_2 (P6) exhibits the lowest response of approximately 0.50. The composite sensors demonstrate enhanced sensitivity [18-20], with P2, P3, P4, and P5 reaching nearly 0.81, 1.17, 1.33, and 1.03, respectively, at 2500 ppm. Among all compositions, P4 ($40SnO_2$:$60TiO_2$) exhibits the highest sensitivity. This improvement can be associated with its smaller crystallite size, increased surface-active sites, and SnO_2–TiO_2 interfacial interactions, which promote CO_2 adsorption and electrical resistance modulation [21-22].

IV. Conclusion:

The SnO_2–TiO_2 composite sensors demonstrated improved CO_2 sensing performance compared with the individual SnO_2 and TiO_2 sensors. Among the investigated compositions, P4 ($40SnO_2$:$60TiO_2$) exhibited the highest sensitivity of approximately 1.33 at 2500 ppm CO_2. Its superior performance is associated with the smallest crystallite size (8.78 nm) and very high porosity with an open, sponge-like network and 20–40 nm particles. These features provide increased surface-active sites and facilitate CO_2 diffusion and adsorption. In addition, SnO_2–TiO_2 interfacial interactions promote charge transfer and resistance modulation, making P4 the most responsive composition in this study at room temperature.

V. Acknowledgment:
The authors sincerely acknowledge Vidya Bharati Mahavidyalaya, Amravati for providing the necessary facilities, resources, and a supportive environment to carry out this research work.

References:

1. Khong Van Nguyen , Bui Ha Trung , Chu Van Tuan , Cong Doanh Sai , Tung Duy Vu , Tran Trung , Giang Hong Thai , Ho Truong Giang and Hoang Thi Hien, Ammonia gas-sensing behavior of uniform nanostructured PPy film prepared by simple-straightforward in situ chemical vapor oxidation, Open Physics **2023**; 21, 1-13.

2. Yawale S. P, Yawale S. S, Lamdhade G. T., Hybrid Composites of Poly (diphenylamine sulfonic acid) and nano-Alumina for Impedimetric Humidity Sensors, Sensors and Actuators A, **2007,** 135, 388–393.

3. Petrov V. V.; Sysoev V. V.; Starnikova A. P.; Volkova M. G.; Kalazhokov Z. K.; Storozhenko V. Y.; Khubezhov S. A.; Bayan E. M. "Synthesis, Characterization and Gas Sensing Study of ZnO–SnO_2 Nanocomposite Thin Films." *Chemosensors,* **2021**, *9* (6): Article 124.

4. Peng Wu, Yi Li, Song Xiao, Junyi Chen, Ju Tang, Dachang Chen, Xiaoxing Zhang, "Interaction Mechanisms of Ammonia and Tin Oxide: A Combined Analysis Using Single Nanowire Devices and DFT Calculations", The Journal of Physical Chemistry 2023, 117, 7, 3520–3526.

5. M. Hjiri, S. Algessair, R. Dhahri, H. B. Albargi, N. Ben Mansour, A. A. Assadi & G. Neri, Ammonia gas sensors based on undoped and Ca-doped ZnO nanoparticles", RSC Advances, **2024**, 14, 5001–5011.

6. Anju Thomas and Kalainathan Sivaperuman, Carbon and cobalt co-doped ZnO thin films for highly sensitive and selective ammonia detection at room temperature, Mater. Adv., **2025**, 6, 629-640

7. Aasim Hussain, Shumaila Akram, Anju Dhillon: Comparative Study of Polypyrrole/Zinc Oxide Nanocomposites Synthesized by Different Methods, Research Gate Publication, **2023**, 601-607.

8. Baruah, S.; Nayak, B.; Puzari, A. "Physicochemical Characterization of SnO_2 Grafted Poly p-Phenylenediamine Hybrid Nanocomposites and Their Enhanced Antibacterial Properties." Journal of Polymer Research, **2021**, 28:120 (page 120).

9. Yang, Y.; Kim, D.-H.; Kim, W.-S.; Kang, T.J.; Lee, B.Y.; Hong, S.; Kim, Y.H.; Hong, S.-H. H_2 sensing characteristics of SnO_2 coated single wall carbon nanotube network sensors. Nanotechnology, **2010**, 21, 215501.

10. Gao, T.; Wang, T.H. Sonochemical synthesis of SnO_2 nanobelt/CdS nanoparticle core/shell heterostructures. Chem. Commun., **2004**, 22, 2558-2559.

11. Han, X.M.; Zhang, B.; Guan, S.K.; Liu, J.D.; Zhang, X.; Chen, R.F. Gassensing properties of SnO_2 nanobelts synthesized by thermal evaporation of Sn foil. J. Alloys Comp., **2008**, 461, L26-L28.

12. Kumar, S.; Peng, Z.C.; Shin, H.; wang, Z.L.; Hesketh, P.J. AC dielectrophoresis of tin oxide nanobelts suspended in ethanol: manipulation and visualization. Anal. Chem., **2010**, 82, 2204-2212.

13. Huang, H.; Lee, Y.C.; Tan, O.K.; Zhou, W.; Peng, N.; Zhang, Q. High sensitivity SnO_2 single-nanorod sensors for the detection of H_2 gas at low temperature. Nanotechnology, **2009**, 20, 115501.

14. Huang, J.; Matsunaga, N.; Shimanoe, K.; Yamazoe, N.; Kunitake, T. Nanotubular SnO_2 templated by cellulose fibers: Synthesis and gas sensing. Chem. Mater., **2005**, 17, 3513-3518.

15. Prabakaran, K.; Sufiyan, K. T. M.; Kumar, S.; et al. "Synthesis of Zinc Oxide and Tin Oxide (ZnO/SnO_2) Nanocomposite for Photoanode Applications in Dye Sensitized Solar Cell." *Journal of Materials Science: Materials in Electronics*, **2024**, vol. 35, p. 1993.

16. Sayali Atkare, Som Datta Kaushik, Shweta Jagtap, Chandra Sekhar, Room - temperature chemiresistive Ammonia sensors based on 2D MXenes and hybrids. Dalton Trans., **2023**, 52, 13831–13851.

17. Jose Carlos Santos-Ceballos, Foad Salehni, Frank Guell Alfonso Romero, Xavier Vilanov, Eduard Llobet, Room-Temperature Ammonia Sensing Using Polyaniline-Coated Laser-Induced Graphene, Sensors, 24, **2024**, 1-16.

18. Y Xiao, Y X Pang, Y Yan, P Qian, H Zhao, S Manickam, Wu T, C H Pang, Synthesis and Functionalization of Graphene Materials for Biomedical Applications: Recent Advances, Challenges, and Perspectives. Adv. Sci., **2023**, 10, 2205292

19. V B Mbayachi, E Ndayiragije, T Sammani, S Taj, E R Mbuta, A U Khan, Graphene Synthesis, Characterization and Its Applications: A Review. Results Chem., **2021**, 3, 100163.

20. Pan, J.; Ganesan, R.; Shen, H.; Mathur, S. Plasma-modified SnO2 nanowires for enhanced gas sensing. J. Phys. Chem. C, **2010**, 114, 8245-8250.

21. Wang, Z.X.; Liu, L. Synthesis and ethanol sensing properties of Fe-doped SnO2 nanofibers. Mater. Lett., **2009**, 63, 917-919.

22. Van Hieu, N.; Kim, H.R.; Ju, B.K.; Lee, J.H. Enhanced performance of SnO_2 nanowires ethanol sensor by functionalizing with La_2O_3. Sens. Actuators B, **2008**, 133, 228-234.